

Direct Electrochemistry of Eugenol at a Glassy Carbon Electrode Modified with Electrochemically Reduced Graphene Oxide

Shijie Wang¹, Ting Zhang¹, Zhe Wang¹, Dong Wang¹, Zhao Wang¹, Mojie Sun^{1*}, Xiaochen Song², Hong Liu³

¹ School of Chemical Engineering, Northeast Electric Power University, 169[#] Changchun Road, Chuanying District, Jilin 132012, China

² School of Mechanical Engineering, Northeast Electric Power University, 169[#] Changchun Road, Chuanying District, Jilin 132012, China

³ Jilin Environmental Monitoring Station, 27[#] Songjiang Road, Changyi District, Jilin 132012, China

*E-mail: smoj@neepu.edu.cn

Received: 3 December 2018 / Accepted: 21 January 2019 / Published: 10 March 2019

An electrochemically reduced graphene oxide modified glassy carbon electrode (ERGO/GCE) was synthesized by direct electrochemical reduction of graphite oxide on a glassy carbon electrode (GCE). The prepared ERGO/GCE shows higher sensitivity to eugenol than the bare GCE due to the large surface area and excellent conductivity, indicating that a direct electrochemical behaviour can be significantly enhanced through electrochemically reduced graphene oxide (ERGO) surface modification. The ERGO/GCE displays a fast response time of less than 5 s and has a detection limit of 5×10^{-7} M, covering a linear range from 5×10^{-6} M to 1×10^{-4} M. As a result, ERGO nanomaterials have potential applications in sensitive eugenol sensors.

Keywords: Eugenol; ERGO; Direct electrochemistry; Sensor

1. INTRODUCTION

It is well known that flavourings are often added to food products for good taste, but some of them can threaten human health [1]. Regulatory authorities have given more attention to even low levels of suspected toxins in food flavourings [2]. Eugenol (4-allyl-2-methoxyphenol) has been widely used in the food flavour as a naturally occurring phenolic compound [3-5], but high doses of eugenol are harmful to humans. It is reported that eugenol, the major component of clove cigarettes, is associated with severe, acute pulmonary illnesses in humans [6-8]. Maralhas et al. reported that eugenol induces chromosomal aberrations in the absence of an exogenous biotransformation system

[9]. However, there is a clear criterion for the highest safe dosage of eugenol according to the International Fragrance Association (IFRA). Therefore, the detection of trace quantities of eugenol is of broad interest [10-12].

Many detecting methods have been developed for several years, such as gas chromatography (GC), gas chromatography/mass spectrometry (GCMS) [13], high-performance liquid chromatography (HPLC) [14] and reverse phase high-performance liquid (RP-HPLC) [15,16]. The above methods display powerful ability but suffer from the obvious disadvantages of expensive instruments, complicated pretreatment and long time for the whole assay. Commonly, electrochemical test methods, which have advantages including easy preparation, high sensitivity and low cost, are widely used in the sensor field, but there are few reports about the electrochemical detection of eugenol. Ciszewski et al. studied the general properties of chemically modified platinum and glassy carbon electrodes (GCEs) based on polymeric films derived from eugenol [17]. This result suggests that eugenol on a GCE shows good electrochemical behaviour. Recently, graphene as a single layer of sp^2 carbon atoms has shown tremendous application potential in electrochemical sensing because of its large surface areas, high conductivity, excellent electrocatalytic activity and good chemical stability [18-24]. For the reasons given above, it is reasonable to propose that a graphene-modified GCE may exhibit a sensitive electrochemical response to eugenol [25-30].

In this work, graphene was fabricated by direct electrochemical reduction of graphite oxide on a GCE. Compared with the chemical reduction method, the electrochemical method displays the advantages of being fast, convenient and easily controllable. The direct electrochemistry of eugenol based on an electrochemically reduced graphene oxide modified GCE (ERGO/GCE) is investigated in detail.

2. EXPERIMENTS

2.1 Materials

Eugenol (98.5% purity, Sinopharm Chemical Reagent Ltd. Co., China), graphite powder (95% purity, 30 μm particle size, Sinopharm Chemical Reagent Ltd. Co., China) and Nafion (5 wt.%, Sigma, U.S.A.) were used as received. Phosphate buffer solutions (PBSs) with different pH values were prepared with Na_2HPO_4 and NaH_2PO_4 . Deionized water was used as the solvent throughout the experiments, and all chemicals used were of reagent grade.

2.2 Preparation of ERGO/GCE.

Graphite oxide (GO) was fabricated from natural graphite powder by the modified Hummers method as reported previously [31]. The graphite oxide powder was exfoliated ultrasonically in deionized water to form a GO suspension solution (1.0 mg mL^{-1}). For every use, 5 mL of GO suspension solution (1.0 mg mL^{-1}) was mixed with 25 μL Nafion. Prior to modification, the surface of the GCE was polished in turn with 0.3 μm and 0.05 μm alumina powders and then ultrasonically

cleaned in water and ethanol in sequence. The well-cleaned electrode was dried at room temperature. The GO-modified glassy carbon electrode (GO/GCE) was prepared by casting 15 μL of the prepared mixture of GO solution and Nafion onto the surface of the GCE and allowing it to dry in air. As the working electrode, the GO/GCE was synthesized by electrochemical reduction of GO on the GCE under a constant potential of -1.3 V in 0.1 M PBS (pH 5) for 60 s. As a result, an electrochemically reduced graphene oxide modified GCE (ERGO/GCE) was obtained.

2.3 Apparatus and measurements

The electrochemical experiments were performed using a CHI660D electrochemical analyser (Shanghai Chenhua Instruments, China) in a conventional three-electrode system, employing an Ag/AgCl electrode, a platinum wire, and the modified GCE (3 mm in diameter) as the reference, counter and working electrodes, respectively. Pure nitrogen was utilized for a thoroughly anaerobic condition. All electrochemical measurements were performed at room temperature (25 °C). Raman spectra were obtained using a Thermo Scientific DXR Raman microscope with a 532 nm DPSS laser and a 50 \times objective (NA = 0.42) (USA).

3. RESULTS AND DISCUSSION

The SEM image of the ultrasonically exfoliated GO in water solution is shown in Fig. 1. The sample exhibits the typical wrinkle morphology of GO [32]. Furthermore, Raman spectroscopy is an important tool for characterizing carbon products. Fig. 2 shows the Raman spectra of pristine graphite (a), GO (b) and electrochemically reduced GO (ERGO) (c). For the spectrum of the pristine graphite, the G band, D band and 2D band are located at 1580 cm^{-1} , 1340 cm^{-1} and 2700 cm^{-1} , respectively. However, the spectrum of GO indicates that the intensity of the D band increases, which suggests a decrease in the size of the in-plane sp^2 domain. This change may be attributed to the extensive oxidation and ultrasonic exfoliation [33]. Furthermore, compared with that of GO, the intensity ratio of bands D and G increases from curve (c), which is probably due to the alteration of structural defects during the electrochemical reduction process [34,35]. At the same time, the decreasing 2D peak intensity reveals that the defects caused by fast electrochemical reduction are difficult to recover in time. The Raman results suggest the successful reduction of GO on GCE, and the ERGO retains the sp^2 -hybridized lattice of graphene.

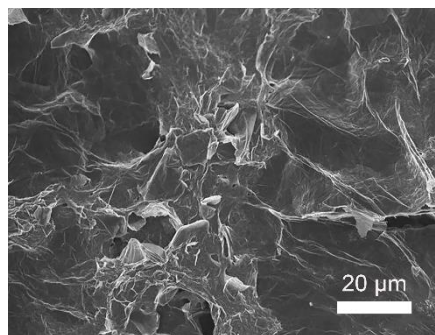


Figure 1. SEM image of graphene oxide.

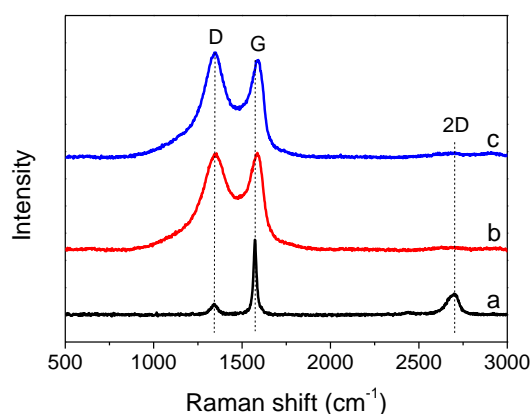


Figure 2. Raman spectra of (a) (pristine graphite,)b(GO and)c(ERGO).

The direct electrochemistry of eugenol on an ERGO/GCE was investigated by cyclic voltammetry, as shown in Fig. 3. The typical cyclic voltammograms (CVs) of ERGO/GCE in 0.1 M PBS (pH 5) with 4.6×10^{-5} M eugenol were obtained, where a well-defined anodic peak P1 at 0.5 V and a cathodic peak P2 at 0.28 V are seen on the first cycle. However, a new peak P3 appears at the potential of 0.3 V on the second cycle. The irreversible peak P1 is assigned to the oxidation of 4-allyl-2-methoxyphenol to 4-allyl-1,2-quinone, and the redox couple of peaks P2 and P3 is ascribed to the reversible redox transition between 4-allyl-1,2-quinone and 4-allyl-1,2-benzenediol. In addition, the current of peak P1 dramatically decreases on the second cycle. This phenomenon may be attributed to the rapid deposition of polymer on the electrode surface [36]. Therefore, in the following experiments, the peak P1 on the first circle is utilized as the characteristic peak to study the direct electrochemistry of eugenol on the ERGO/GCE.

The ERGO/GCE was prepared by electrochemical reduction of exfoliated GO on a GCE at -1.3 V in 0.1 M PBS (pH 5) for different times, and the CVs were obtained in 0.1 M PBS (pH 5) with 4.6×10^{-5} M eugenol. As shown in Fig. 4, as the reducing time increases, the oxidation peak current increases and reaches the maximal height when the exfoliated GO is reduced for 60 s; afterwards, the peak current decreases with time, indicating that the covering GO could not be reduced completely when the reduction time was less than 60 s. Therefore, 60 s is the best electrochemical reduction time

for the most sensitive peak current to eugenol.

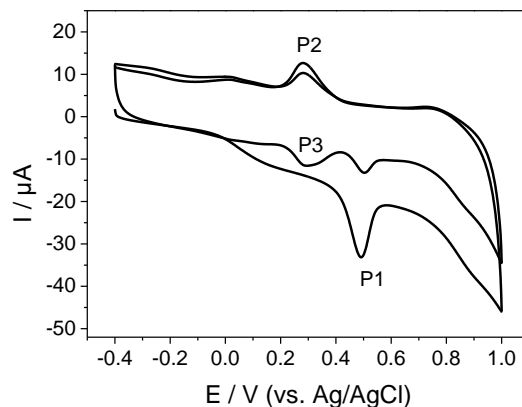


Figure 3. CVs of the ERGO/GCE in 0.1 M PBS (pH 5) with 4.6×10^{-5} M eugenol for two circles. Scan rate: 50 mV s^{-1} .

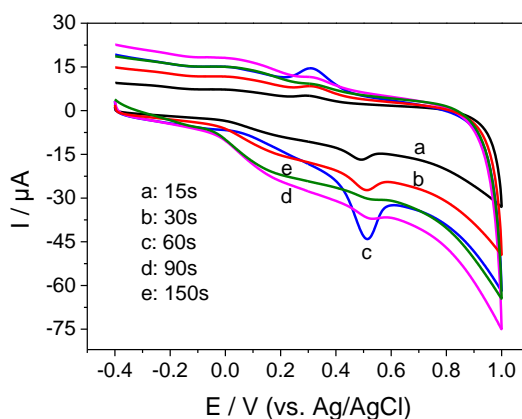


Figure 4. CVs of the ERGO/GCE prepared by electrochemical reduction of GO at -1.3 V for (a) 30 s, (b) 45 s, (c) 60 s, (d) 90 s and (e) 150 s in 0.1 M PBS (pH 5) with 4.6×10^{-5} M eugenol. Scan rate: 50 mV s^{-1} .

Fig. 5 shows the CVs of the GCE and ERGO/GCE in 0.1 M PBS (pH 5) with 4.6×10^{-5} M eugenol at a scan rate of 50 mV s^{-1} . There is a weak oxidation peak current for the GCE; however, the oxidation peak current for the ERGO/GCE has an approximately 10 times higher peak current than that on the bare GCE, indicating that the ERGO film offers a place for faster electron transfer and improves the direct electron transfer between eugenol and the surface of electrode. This result is ascribed to the excellent conductivity and the large surface area of the ERGO film, making it a sensitive promoter for electrochemical sensing processes [37].

The CVs of the ERGO/GCE in 0.1 M PBS with 4.6×10^{-5} M eugenol of different pH values were measured. As shown in Fig. 6 (A), the ERGO/GCE exhibits a strong dependence on the solution pH value. The peak current increases significantly from pH 4 to pH 5 and decreases slightly with increasing pH. At the same time, there are negative shifts in the characteristic peak potentials in the pH range of 4.0-8.0. The oxidation peak potential of eugenol linearly decreases with increasing pH, as

shown in Fig. 6 (B). These results suggest that the hydrogen ion is involved in the oxidation reaction of eugenol on the ERGO/GCE [38]. Apparently, the maximum peak current is observed at pH 5, indicating that eugenol shows the highest sensitivity on the ERGO/GCE around the pH 5 value.

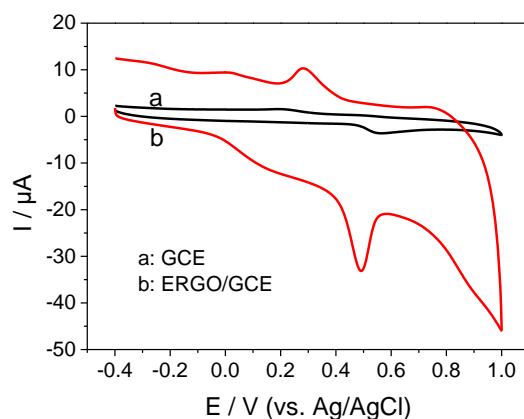


Figure 5. CVs of the (a) GCE and (b) ERGO/GCE in 0.1 M PBS (pH 5) with 4.6×10^{-5} M eugenol. Scan rate: 50 mV s^{-1} .

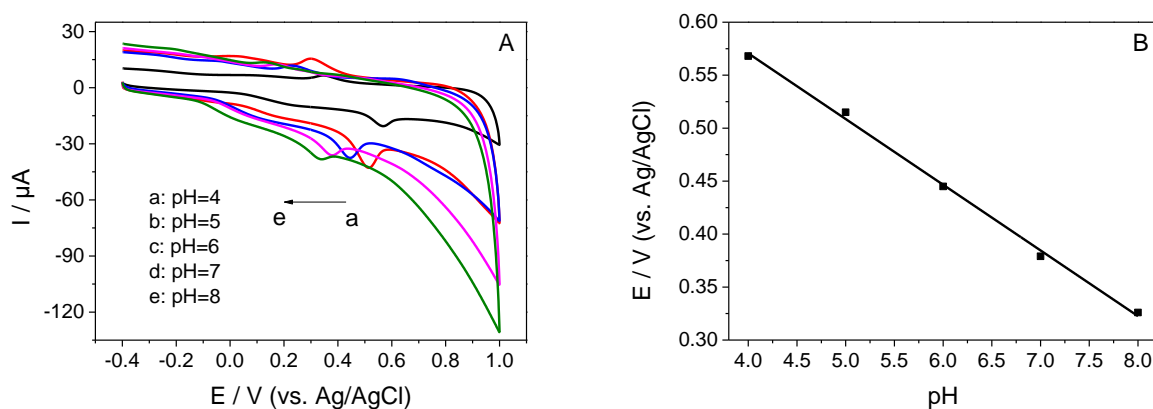


Figure 6. (A) CVs of the ERGO/GCE in 0.1 M PBS with 4.6×10^{-5} M eugenol of different pH values: (a) pH 4, (b) pH 5, (c) pH 6, (d) pH 7 and (e) pH 8. Scan rate: 50 mV s^{-1} . (B) Plot of formal potentials versus pH values.

The effect of scan rate on the ERGO/GCE in 0.1 M PBS (pH 5) with 4.6×10^{-5} M eugenol was studied by evaluating the CVs. Fig. 7 (A) shows the positive shift of the oxidation peak potentials as the scan rate increases due to the irreversible oxidation reaction of eugenol. Furthermore, an increasing linear relationship between the characteristic peak currents and the $(\text{scan rate})^{1/2}$ covering the scan rate of $10\text{-}150 \text{ mV s}^{-1}$ is shown in Fig. 7 (B), which indicates that the current is controlled by a semi-infinite linear diffusion with the scan rate, according to the literature [39].

The CVs of the ERGO/GCE in 0.1 M PBS (pH 5) with different eugenol concentrations were obtained. As shown in Fig. 8 (A), the oxidation current from the ERGO/GCE CVs increases with increasing eugenol concentration at approximately 0.5 V. Furthermore, Fig. 8 (B) displays the

amperometric response of different concentrations of eugenol at the ERGO/GCE with an applied potential of 0.5 V. During the experiment, the concentration of eugenol was increased by successive additions of 50 μL 1.0 mM eugenol into 10 mL 0.1 M PBS (pH 5) with stirring every 40 s. The ERGO/GCE shows a fast response time, reaching a stable plateau in less than 5 s. Such a rapid response is due to the ERGO film, which could provide a fast electron transfer process [40]. In addition, as the calibration curve shows in Fig. 8 (C), the response current exhibits a good linear relationship with the eugenol concentration ranging from 5.0×10^{-6} M to 1.0×10^{-4} M, with a correlation coefficient of 0.999. At the same time, the detection limit is determined to be 5.0×10^{-7} M.

The performance of the ERGO/GCE was compared with the other methods and sensors in Table 1 [25,41-44]. As a result, the ERGO/GCE shows fast response time, good linear range and lower LOD, as well as easier preparation. In addition to the large specific surface area and good electron transfer performance of ERGO itself, the excellent performance of the ERGO/GCE is also attributed to the enhanced synergistic effect of the ERGO and GCE during the electrochemical reduction of graphene oxide. In conclusion, an ERGO nanomaterial was successfully prepared for the detection of trace amounts of eugenol, and it has potential application in sensitive eugenol sensors.

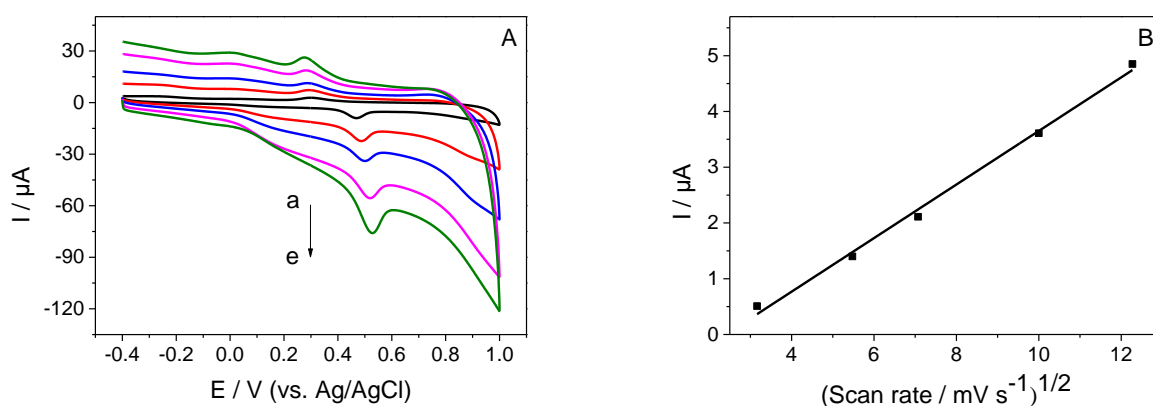


Figure 7. (A) CVs of the ERGO/GCE in 0.1 M PBS (pH 5) with 4.6×10^{-5} M eugenol at a scan rate of (a) 10 mV s^{-1} , (b) 30 mV s^{-1} , (c) 50 mV s^{-1} , (d) 100 mV s^{-1} and (e) 150 mV s^{-1} . (B) Plot of the peak current against the scan rate.

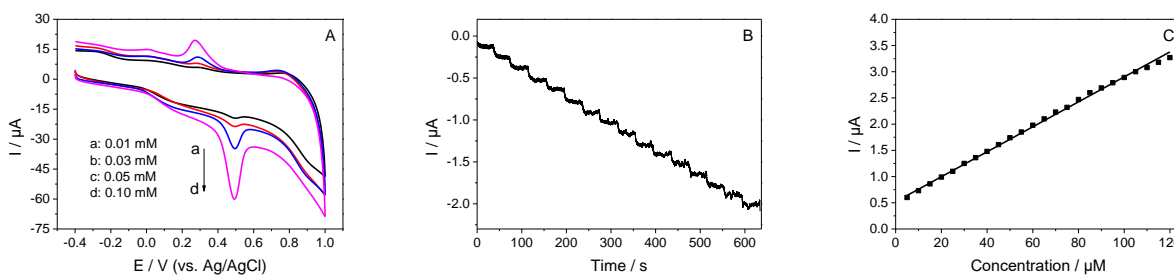


Figure 8. (A) CVs of the ERGO/GCE in 0.1 M PBS (pH 5) with (a) 0.01 mM, (b) 0.03 mM, (c) 0.05 mM and (d) 0.10 mM eugenol. Scan rate: 50 mV s^{-1} . (B) Amperometric response of eugenol at the ERGO/GCE with additions of 50 μL 1.0 mM eugenol into 10 mL 0.1 M PBS (pH 5) with stirring every 40 s. Applied potential: 0.5 V. (C) Plot of response current vs. eugenol concentration.

Table 1. Comparison of the proposed ERGO/GCE for determination of eugenol with other methods and sensors.

Methods & Sensors	LOD (μM)	Linear range (μM)	References
GC-FID	1.22	1.89-3806	[41]
RP-HPLC-UV	3.11	0-9146	[42]
PVC-Graphite/Electrode	1.01	3.04-182.7	[43]
GN-CNTs-IL	0.1	0.50-20.0	[25]
CeO ₂ -CPB/GCE	0.019	0.075-75.0	[44]
ERGO/GCE	0.50	5.0-100.0	This work

4. CONCLUSIONS

In this work, the direct electrochemical behaviour of eugenol at an ERGO/GCE in aqueous solution was studied. The results indicate that the ERGO/GCE shows higher sensitivity to eugenol than the bare GCE due to the large surface area and excellent conductivity. The best conditions for the highest sensitivity to eugenol using the ERGO/GCE were further explored at room temperature. The ERGO/GCE, which is obtained by the electrochemical reduction of exfoliated GO coated on a GCE at 0.5 V for 60 s, exhibits the best current response to eugenol in the solution of pH 5. In addition, there is a good linear relationship with the eugenol concentration ranging from 5.0×10^{-6} M to 1.0×10^{-4} M, with fast response times of less than 5 s. The detection limit is determined to be 5.0×10^{-7} M, which is 100 times lower than the IFRA standards for eugenol in flavourings (9.6-100 mg kg⁻¹) [45]. The results reported above demonstrate that ERGO nanomaterials are promising for fabricating eugenol sensors.

References

1. J.B. Jones, M. Provost, L. Keaver, C. Breen, M.J. Ludy, R.D. Mattes, *American Journal of Clinical Nutrition*, 99 (2014) 490.
2. H. Devaraj, S. Niranjali, M. Raveendran, *Bulletin of Environmental Contamination & Toxicology*, 49 (1992) 306.
3. C.I. Heck, E.G.D. Mejia, *Journal of Food Science*, 72 (2007) R138.
4. A. Steffen, J. Pawliszyn, *Journal of Agricultural & Food Chemistry*, 44 (1996) 2187.
5. X. Yang, T. Peppard, *Journal of Agricultural & Food Chemistry*, 42 (1994) 1925.
6. T.L. Guidotti, L. Laing, U.B. Prakash, *Western Journal of Medicine*, 151 (1989) 220.
7. E.J. Lavoie, J.D. Adams, J. Reinhardt, A. Rivenson, D. Hoffmann, *Archives of Toxicology*, 59 (1986) 78.
8. G.M. Polzin, S.B. Stanfill, C.R. Brown, D.L. Ashley, C.H. Watson, *Food & Chemical Toxicology*,

- 45 (2007) 1948.
9. A. Maralhas, A. Monteiro, C. Martins, M. Kranendonk, A. Laires, J. Rueff, A.S. Rodrigues, *Mutagenesis*, 21 (2006) 199.
 10. C.D. Elvidge, Z. Chen, D.P. Groeneveld, *Remote Sensing of Environment*, 44 (1993) 271.
 11. S. Kermasha, M. Goetghebeur, J. Dumont, *LWT-Food Science and Technology*, 27 (1994) 578.
 12. J.L. Pinkus, L.S. Goldman, *Journal of Chemical Education*, 54 (1977) 380.
 13. D.E. Huff, Trace Detection of Isoeugenol of Local Water Samples via GC and GC/MS, ProQuest Dissertations Publishing, (2016)Ann Arbor, Michigan, U.S.A..
 14. Z. Aydoğmuş, G. Yıldız, E.M. Yılmaz, H.Y. Aboul-Enein, *Graphene Technology*, 3 (2018) 1.
 15. F. Sotoudegan, M. Amini, M. Faizi, R. Aboofazeli, *Iranian Journal of Pharmaceutical Research*, 16 (2017) 471.
 16. Z. Zeng, Z. Ji, N. Hu, B. Bai, H. Wang, Y. Suo, *J Chromatogr B Analyt Technol Biomed Life Sci*, 1064 (2017) 151.
 17. A. Ciszewski, G. Milczarek, *Electroanalysis*, 13 (2015) 860.
 18. Y. Chen, L. Li, J.J. Zhu, Carbon and Graphene Dots for Electrochemical Sensing, John Wiley & Sons Ltd, (2017)Hoboken, New Jersey, U.S.A..
 19. C.J. Venegas, E. Yedinak, J.F. Marco, S. Bollo, D. Ruiz-León, *Sensors & Actuators B: Chemical*, 250 (2017) 412.
 20. X. Li, H. Zhao, L. Shi, X. Zhu, M. Lan, Q. Zhang, Z.H. Fan, *Journal of Electroanalytical Chemistry*, 784 (2017) 77.
 21. A.R. Thirupathi, B. Sidhureddy, W. Keeler, A. Chen, *Electrochemistry Communications*, 76 (2017) 42.
 22. T.R. Madhura, P. Viswanathan, G.G. Kumar, R. Ramaraj, *Journal of Electroanalytical Chemistry*, 792 (2017) 15.
 23. L.A. Mercante, M.H.M. Facure, R.C. Sanfelice, F.L. Migliorini, L.H.C. Mattoso, D.S. Correa, *Applied Surface Science*, 407 (2017) 162.
 24. Y. Tian, Z. Wei, K. Zhang, S. Peng, X. Zhang, W. Liu, K. Chu, *Sensors & Actuators B: Chemical*, 241 (2017) 584.
 25. L. Yang, F. Zhao, B. Zeng, *Electrochimica Acta*, 210 (2016) 293.
 26. B. Xu, B. Zhang, L. Yang, F. Zhao, B. Zeng, *Electrochimica Acta*, 258 (2017) 1413.
 27. G. Yildiz, Z. Aydogmus, M.E. Cinar, F. Senkal, T. Ozturk, *Talanta*, 173 (2017) 1.
 28. Q. Feng, K. Duan, X. Ye, D. Lu, Y. Du, C. Wang, *Sensors & Actuators B: Chemical*, 192 (2014) 1.
 29. M. Parsaei, Z. Asadi, S. Khodadoust, *Sensors & Actuators B: Chemical*, 220 (2015) 1131.
 30. L.J. Liu, X. Gao, P. Zhang, S.L. Feng, F.D. Hu, Y.D. Li, C.M. Wang, *Journal of Analytical Methods in Chemistry*, 2014 (2014) 424790.
 31. G. Eda, G. Fanchini, M. Chhowalla, *Nat. Nanotechnology*, 3 (2008) 270.
 32. D.A. Dikin, S. Stankovich, E.J. Zimney, R.D. Piner, G.H.B. Dommett, G. Evmenenko, S.T. Nguyen, R.S. Ruoff, *Nature*, 448 (2007) 457.
 33. S. Stankovich, D.A. Dikin, R.D. Piner, K.A. Kohlhaas, A. Kleinhammes, Y. Jia, Y. Wu, S.T. Nguyen, R.S. Ruoff, *Carbon*, 45 (2007) 1558.
 34. A. Gupta, G. Chen, P. Joshi, S. Tadigadapa, P.C. Eklund, *Nano Lett*, 6 (2006) 2667.
 35. R. Li, X. Dong, C. He, Z. Liu, L. Huang, Y. Yang, *Int. J. Electrochem. Sci.*, 12 (2017) 144.
 36. A.A. Ensafi, E. Khnoddami, B. Rezaei, H. Karimi-Maleh, *Colloids & Surf. B: Biointerfaces*, 81 (2010) 42.
 37. M. Pumera, *Chem. Soc. Rev.*, 39 (2010) 4146.
 38. D. Nematollahi, H. Shayani-Jam, M. Alimoradi, S. Niroomand, *Electrochimica Acta*, 54 (2009) 7407.
 39. X. Ye, Y. Du, D. Lu, C. Wang, *Analytica Chimica Acta*, 779 (2013) 22.
 40. X. Zheng, H. Yu1, S. Yue, R. Xing, Q. Zhang, Y. Liu, B. Zhang, *Int. J. Electrochem. Sci.*, 13 (2018) 1.

41. B. Yu, S. Lai, Q. Tan, *Chemical & Pharmaceutical Bulletin*, 54 (2006) 114.
42. Y. Li, Z. Sun, P. Zheng, *Chromatographia*, 60 (2004) 709.
43. M. Luque, A. Ríos, M. Valcárcel, *The Analyst*, 125 (2000) 1805.
44. G. Ziyatdinova, E. Ziganshina, S. Romashkina, H. Budnikov, *Electroanalysis*, 29 (2017) 1197.
45. The IFRA Standards on http://ifraorg.org/en-us/library_1/s0/p11.

© 2019 The Authors. Published by ESG (www.electrochemsci.org). This article is an open access article distributed under the terms and conditions of the Creative Commons Attribution license (<http://creativecommons.org/licenses/by/4.0/>).